Acidic Fibroblast Growth Factor in the Developing Rat Embryo

Ya-Min Fu, Paolo Spirito, Zu-Xi Yu, Sadatoshi Biro, Joachim Sasse,‡ Jun Lei, Victor J. Ferrans,* Stephen E. Epstein, and Ward Casscells

Cardiology Branch and *Ultrastructure Section of the Pathology Branch, National Heart, Lung, and Blood Institute, National Institutes of Health, Bethesda, Maryland 20892; and ‡Shriner's Hospital for Crippled Children, Tampa, Florida 33612

Abstract. Compared to basic fibroblast growth factor (bFGF), a widely distributed, broad spectrum mitogen and mesoderm inducer, acidic fibroblast growth factor (aFGF) is reported to have an essentially neural distribution and to be undetectable in the early embryo. In the present investigation, we used immunoblotting and immunochemistry to assess the cellular and tissue distributions of aFGF and bFGF in 11–20-d rat embryos.

Immunoblotting of crude and heparin-bound embryo extracts revealed faint bands at the expected 17–18-kD and predominant bands at an apparent molecular mass of 26 to 28-kD (despite reducing conditions) using multiple specific antibodies for aFGF and bFGF. Pretreatment with 8 M urea yielded 18–20-kD aFGF and bFGF and some 24–26-kD bFGF. Immunoreactivity for both aFGF and bFGF was positive and similar in the cytoplasm, nuclei, and extracellular matrix of cells of neuroectodermal and mesodermal origin, while it was negative in endoderm-derived cells. The distribution of immunoreactive aFGF and bFGF also showed changes during development that were associated with the process of cellular and tissue differentiation. For example, intensity and extent of immunoreactivity for both peptides progressively increased in the middle layer of the spinal cord with increasing differentiation of the neural cells. The immunostaining patterns were very similar for aFGF and bFGF for each organ and at each stage. In conclusion, high molecular mass forms of immunoreactive aFGF and bFGF are present in the rat embryo. Acidic FGF and bFGF are both widely distributed in tissues of neuroectodermal and mesodermal origin, and their distribution was very similar.

Basic fibroblast growth factor (bFGF)[1] and acidic fibroblast growth factor (aFGF, also known as heparin-binding growth factor 1) are closely related polypeptides that have a widespread distribution in tissues and have been extremely well conserved throughout evolution, a feature that suggests physiological importance (1–3, 5, 8, 26). However, the precise biological functions of bFGF and aFGF in vivo remain largely unknown. In vitro studies have shown that these two peptides have regulatory effects on many cellular functions, such as proliferation, differentiation, matrix formation, and cell movement (3, 5, 26, 36). Because each of these functions is of critical importance during embryonic development, these growth factors could play a major role in embryogenesis. Using biochemical and immunological methods, bFGF and its messenger RNA have been identified in amphibian oocytes and embryos and its mesoderm-inducing effect has been demonstrated (35–37, 55, 56). Limited immunohistochemical studies in chicken and rat embryos have shown that the presence of bFGF is associated with developmental events such as angiogenesis and early muscle morphogenesis (25, 34, 52). For aFGF, no embryonic distribution has been reported (9, 25, 30, 34).

1. *Abbreviations used in this paper*: aFGF, acidic fibroblast growth factor; bFGF, basic fibroblast growth factor.

In the present study, we have used Western blot techniques to investigate the expression of aFGF and bFGF in whole rat embryos. We have also used immunohistochemical techniques to define the cellular and tissue distribution of aFGF in embryos at different stages of development (from 11 to 20 d of gestation), and to compare the distribution of aFGF with that of bFGF.

Materials and Methods

We studied 60 Sprague-Dawley rat embryos ranging from 11 to 20 d of gestation (crown-to-rump length, 2–23 mm) as described (23, 29).

Extraction of aFGF and bFGF from Rat Embryos

After dissecting the placenta and freezing in liquid nitrogen, embryos were homogenized for 30 s using a Polytron (Brinkmann, Luzern, Switzerland) in 8–10 vol of 0.5 M NaCl, 20 mM Tris, 3 mM EDTA, 0.2 mM PMSF, pH 6.5 at 4–10°C. The homogenized tissue underwent three freeze–thaw cycles and was then centrifuged at 48,000 *g* for 120 min. The clear supernatant (crude extract) was used for Western blot analysis and bioassays.

The supernatant (1–2 ml), in 0.5 M NaCl, was also batch absorbed overnight with 0.4 ml heparin-Sepharose beads, while gently rocking. After being transferred to a column, the beads were washed with 0.6 M NaCl in 10 mM Tris, and were eluted with a step gradient of 1.1, 1.5, and 3.0 M NaCl in 10 mM Tris. Aliquots were obtained for Western blot analysis and bioassays.

Antibodies

For identification of aFGF, two polyclonal antibodies and a monoclonal antibody were used. The two polyclonal antibodies (#63 and #119) were raised in rabbit against human/bovine aFGF (residues 65–97, SIG . . . NEE). This 33-amino acid region of aFGF is only 33% homologous to hst (58)/K-FGF (11), FGF-5 (62), and FGF-6 (40). We found cross-reactivity of these two antibodies with bFGF is 1% in Western blots. The monoclonal antibody against bovine aFGF (Upstate Biotechnology Inc., Lake Placid, NY) recognizes the tyrosine 111 to lysine 126 region of aFGF, a region with only 12–25% homology with int-2 (12), hst/KFGF (11, 58), and FGF6 (40), and has very little cross-reactivity with bFGF (<1% in Western blots, in our laboratory). The stock concentrations for these antibodies were the following: 28 mg/ml for antibody #63; 34 mg/ml for #119; and 1 mg/ml for the monoclonal antibody.

For identification of bFGF, three rabbit polyclonal antibodies and five monoclonal antibodies were used. One (#773) was raised against the first 24 amino acids of bovine bFGF, a region with 100% homology to human bFGF and 96% homology to rat bFGF, but no homology to the predicted amino acid sequences of int-2, hst/K-FGF, FGF-5, FGF-6, or KGF (17). A second (#967) was raised against human recombinant bFGF (whole molecule); and a third was raised against bFGF COOH-terminal residues AIL . . . SAK. The antibodies #773 and #967 are IgG purified and were kindly provided by Dr. Andrew Baird (The Whittier Institute, La Jolla, CA). The cross-reactivity to aFGF of antibody #773 is 2% in Western blots, 0.1% in RIA, and those of antibody #967 and the COOH-terminal antibody are <1% in Western blots. The five monoclonal antibodies were prepared from BALB/c mice using the hybridoma technique; two of them (mAb #12 and #78) recognize their epitope located at the first nine residues of the human recombinant bFGF, a region with no homology to other FGF family members; the two remaining monoclonal antibodies (mAb #52 and #98) recognize the site between the amino acid residues 14 and 40. These four monoclonal antibodies were the kind gift of the Pharmaceutical Group, Takeda Chemical Industries, Ltd., Osaka, Japan (54). The last monoclonal antibody was antibovine basic FGF type II antibody from Upstate Biotechnology Inc., Lake Placid, NY (cat. No. 05-118). The immunogen for this antibody is purified bovine brain bFGF. This antibody is highly specific for bFGF from bovine human, rat, and mouse source and does not cross-react with aFGF. Each of these monoclonal antibodies showed high specificity, without detectable binding to aFGF in Western blots, in our laboratory. The stock concentrations for these antibodies were the following: 2 mg/ml for antibodies #773 and #967; 18.6 mg/ml for mAb #12; 2.4 mg/ml for mAb #78; 4.9 mg/ml for mAb #52; 5.8 mg/ml for mAb #98; and 2 mg/ml for mAb antibovine bFGF type II.

Western Blot Analysis for aFGF and bFGF

Crude extracts and column fractions were subjected to SDS-PAGE in 4–20 or 10–20% gradient gels and then transferred to nitrocellulose membrane (0.05 μm; Schleicher & Schuell, Inc., Keene, NH) by electrophoretic transfer (Polyblot Transfer System, Model SBD-1000; American Bionetics, Emeryville, CA). To investigate the multiple forms of FGFs, we used Laemmli buffer with and without 8 M urea (to break up potential aggregates) in a stacking gel buffer of 0.0625 M Tris, SDS stock 1%, and dithiothreitol 15 mM. The samples were kept at room temperature 1 h, then 4°C overnight, and boiled before loading onto SDS-PAGE. We also used the adult rat tissue extract as a control. After transfer and blocking of the nonspecific protein-binding sites with 3% dry milk in TBS, the nitrocellulose membrane was incubated with different antibodies at suitable dilutions (1:500 for the monoclonal antibody for aFGF, 1:1,000 for the other antibodies) in wash buffer (10 mM Tris-HCl, pH 8.0, 0.15 M NaCl, 0.05% Tween-20) overnight at 4°C. Antigen–antibody complexes were visualized by incubating the membrane with suitable secondary antibodies and developing it by ProtoBlot Western Blot AP System (Promega, Madison, WI).

Western blot analyses with a preabsorbed monoclonal antibody and a polyclonal antibody for aFGF and bFGF (COOH-terminal) were used to verify the immunospecificity of the staining.

Mitogenicity Assay of Embryo Extracts

BALB/c/3T3 mouse fibroblasts were subcultured and used for determination of growth factor activity, as previously described in detail by Hauschka et al. (28). In brief, Costar 96-well plates were seeded with 1×10^5 cells/well in 200 μl of DMEM and grown for 10 d in 5% CO_2, 95% air incubator at 37°C. Different fractions of embryo extracts were eluted through heparin-Sepharose columns at 1.1, 1.5, and 3.0 M NaCl, and were added to the wells 10 d after cell seeding. Without changing the original plating medium, 2 μl of test substances and 1 μCi of [^{3}H]thymidine in 10 μl of PBS were added to each well. After 48 h of incubation, cells were harvested and radioactivity was measured using a liquid scintillation analyzer (1500 TRI-CARB; Packard Instrument Co., Downers Grove, IL). The background was 1,600–2,200 cpm/well; maximal serum stimulation was 10–15-fold above background.

Immunohistochemistry

The distributions of aFGF and bFGF were investigated by immunohistochemical staining in both sagittal sections and cross-sections of whole rat embryos at 11–20 d of gestation. In each embryo, one sagittal section and three to four cross-sections at the level of the brain, heart, and kidneys were obtained. Embryos were fixed in 4% paraformaldehyde in 0.1 M phosphate buffer, pH 7.4, overnight at 4°C. After dehydration through a graded series of ethanol solutions, several embryos were embedded in one paraffin block to reduce the interassay variability. Sections from each block (6 μm thick) were stained with H & E, Masson and Yajima (periodic acid-methenamine silver staining) methods, for routine morphological evaluation. Sections were immunostained using the following steps: (*a*) blocking of endogenous peroxidase with 3% hydrogen peroxide in methanol (30 min); (*b*) treatment with 2 mg/ml hyaluronidase Type IV-S (No. H-3884; Sigma Chemical Co., St. Louis, MO) in 0.1 M acetate buffer, pH 5.1 (15 min); (*c*) blocking of nonspecific protein binding with 5% goat serum in 50 mM Tris buffer at pH 7.4 (1 h); (*d*) incubation with primary antibodies, at suitable dilution at 4°C overnight (for aFGF, 1:1,000 for the polyclonal antibody #63, 1:500 for the polyclonal antibody #119, and 1:400 for the monoclonal antibody; for bFGF, dilutions were 1:500 for each antibody used; (*e*) incubation with peroxidase-labeled affinity-purified goat anti-rabbit IgG for the polyclonal antibodies (Vector Laboratories, Inc., Burlingame, CA), and incubation with peroxidase labeled affinity-purified horse anti-mouse IgG for the monoclonal antibody (Vector Laboratories, Inc.) (1 h); (*f*) treatment with 0.25 mg/ml diaminobenzidine (Sigma Chemical Co.) in 0.05 M Tris-HCl buffered saline containing 0.01% hydrogen peroxide (10 min); (*g*) counterstaining with 1% methyl green solution (2 min). The buffer solution used for rinsing after each step consisted of 0.01 M Tris-HCl buffered saline and 0.25% Brij-35 (Sigma Chemical Co.), at pH 7.4. All steps, except when otherwise specified, were performed at room temperature.

Immunohistochemical Controls for aFGF and bFGF

No immunostaining was seen in sections after the following immunohistochemical control procedures: (*a*) omission of the primary antibody and incubation with normal rabbit serum at the same (or more concentrated) dilutions used for the primary antibody; (*b*) omission of the primary antibody and incubation with 2% normal goat serum; and (*c*) omission of the primary antibody and incubation with nonimmune mouse IgG at the same (or more concentrated) dilutions used for the primary antibody.

In addition, specificity of immunostaining was confirmed for each antibody by incubation with primary antibody preabsorbed by its corresponding growth factor as described below. Two different procedures were used for absorption of each antibody for aFGF and bFGF. (*a*) After blocking of nonspecific protein binding with 5% goat serum in 50 mM Tris buffer at pH 7.4 (1 h), sections were incubated with preabsorbed antibody at 4°C overnight. Preabsorbed antibody was obtained as follows: antibody at suitable dilutions (total volume 0.3 ml) was incubated with heparin-Sepharose beads saturated with 100–200 μg of aFGF or bFGF, at 4°C overnight. Supernatant was used as preabsorbed antibody. (*b*) After blocking of nonspecific protein binding, as in *a*, specific blocking of FGFs binding sites was obtained as follows. Sections were incubated with 50–100 μg/ml of human recombinant aFGF or bFGF, as appropriate, in 0.2 ml of 2% goat serum, at room temperature for 1 h and subsequently at 4°C for 2 h. Then, sections were incubated with primary antibody. For each antibody, and with each procedure, no immunostaining was seen in sections. Heparin-Sepharose beads alone (without aFGF or bFGF) did not deplete the antibodies of tissue reactivity.

Results

Identification of aFGF and bFGF in Rat Embryos

Western blot analysis for aFGF and bFGF was performed in embryo crude extracts and heparin-bound material obtained at different stages of development (days 16, 17, and 18). A

monoclonal and two polyclonal antibodies for aFGF, and three polyclonal and five monoclonal antibodies for bFGF, were used as Western blotting reagents. For aFGF, at each stage and with each antibody, a band with a molecular mass of ~26 kD was detected (Fig. 1), as well as a fainter band at 18–20 kD. A faint band of 52 kD, perhaps a doublet of 26-kD aFGF, can also be detected. These bands were completely suppressed by adding human recombinant aFGF, thus suggesting specificity of antibody binding. After being boiled in Laemmli buffer with 8 M urea (to more effectively denature and break up aggregates), the 26-kD band became fainter and 18- and 20-kD immunoreactive bands became more intense. By contrast, only 18-kD immunoreactive aFGF was detected in adult rat brain extract (Fig. 1). For bFGF, at each stage and with each antibody used, a doublet or a triplet with a molecular mass from 24 to 28 kD was identified (Fig. 2), as well as the expected (but fainter) band at 17–18 kD. Bands were significantly suppressed by adding human recombinant bFGF. As with aFGF, after boiling in 8 M urea with Laemmli buffer, the 28-kD immunoreactive bFGF band became fainter, and 24-, 22-, and 18-kD bands became more intense. Although the 18-kD immunoreactive bFGF is the predominant form in adult rat brain extracts, 24- and 26-kD immunoreactive bFGF also were detected (Fig. 2).

Mitogenic Activity of Embryo Extracts

The mitogenic activity of embryo extracts is shown in Fig. 3. Mitogenic activity for 3T3 fibroblasts was present in fractions that eluted from heparin-Sepharose columns 1.1 and 1.5 M NaCl, which is consistent with the heparin affinity of aFGF and bFGF, respectively. Crude extracts also showed mitogenic activity for 3T3 cells (Fig. 3). Western blots demonstrated that the 1.1-M fractions contained both aFGF and bFGF.

Immunohistochemical Localization of aFGF

The two polyclonal antibodies and the monoclonal antibody to aFGF used in this study showed a similar pattern of staining in the rat embryos, with specific tissue distribution of immunohistochemically detectable aFGF (Figs. 4–7). Immunoreactive aFGF was identified in tissues of neuroectodermal and mesodermal origin. In addition, the distribution of aFGF showed progressive changes during development both in the neuroectodermal and mesodermal tissues, and such changes appeared to be associated with tissue differentiation. At the cellular level, staining was localized in the cytoplasm, as well as the extracellular matrix. Faint staining was also noted in some nuclei. The pattern of immunostaining in individual organs (described below) was virtually identical for aFGF and bFGF.

Central Nervous System. In the spinal cord, the pattern of immunoreactivity for aFGF was highly specific and showed progressive and consistent changes from earlier to later stages of embryonic development. The neuroepithelial cells that are adjacent to the spinal canal and actively proliferating showed no immunoreactivity throughout development (Fig. 5, *c* and *d*, and 6, *c* and *d*). The mantle zone (middle layer) showed increasingly more intense staining, from earlier

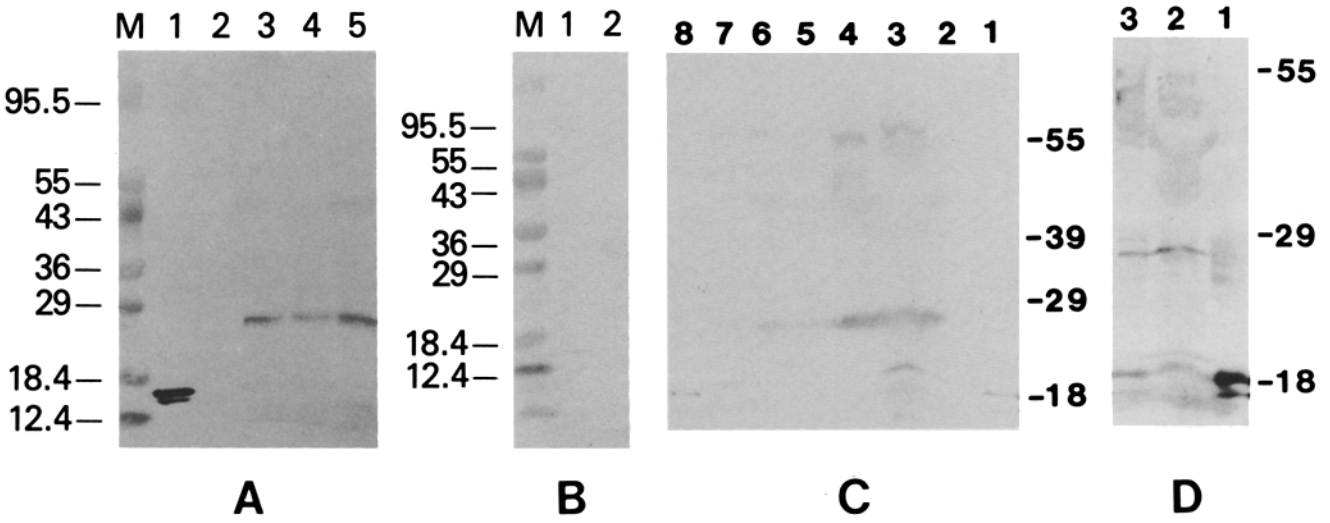

Figure 1. Western blot analysis of rat embryo extracts for aFGF. (*a*) Incubated with anti-aFGF monoclonal antibody (mAb). Lane *M*, molecular mass standards; lane *1*, human recombinant aFGF (hraFGF) 100 ng; lane *2*, human recombinant bFGF (100 ng); lanes *3–5*, crude extracts of 16-, 17- and 18-d embryo; 26-kD bands predominate with faint immunoreactivity at 12–16 kD. (*b*) Incubated with the same antibody preabsorbed with aFGF; lane *1*, hraFGF (100 ng); lane *2*, crude extract of 16-d embryo, no detectable bands. (*c*) Incubated with anti-aFGF mAb; lane *1*, bovine aFGF (50 ng); 18- and 16-kD bands are shown; lane *2*, hrbFGF (50 ng); lane *3*, crude extract of 16-d embryo treated with Laemmli buffer plus 8 M urea to dissociate aggregates; lane *4*, same as in lane *3*, treated with Laemmli buffer; lane *5*, 1.1 M NaCl column eluate from 17-d embryo treated with Laemmli buffer; lane *6*, 1.1 M NaCl column eluate from 16-d embryo treated with Laemmli buffer; lane *7*, same fraction as in lane *6*, treated with Laemmli buffer with 8 M urea; lane *8*, 1.1 M NaCl column eluate from adult rat brain. In all embryo extracts, 26–28-kD bands predominate with faint 18–20 and 55 kD (dimer) immuno-reactivity. After being treated in buffer with 8 M urea, 18- and 20-kD bands predominate and 26–28-kD bands are faint. Only 18-kD band is detected in adult rat brain extract. (*d*) Incubated with anti-aFGF polyclonal Ab #119. Lane *1*, bovine aFGF (25 ng), 18- and 16-kD bands are shown; lane *2*, 1.1 M NaCl column fraction from 16-d embryo treated with Laemmli buffer, intense 28-kD band and fainter 18–20-kD bands are shown; lane *3*, same fraction as in lane *2*, treated with Laemmli buffer with 8 M urea, 28-kD band becomes fainter and 18-kD band becomes more intense.

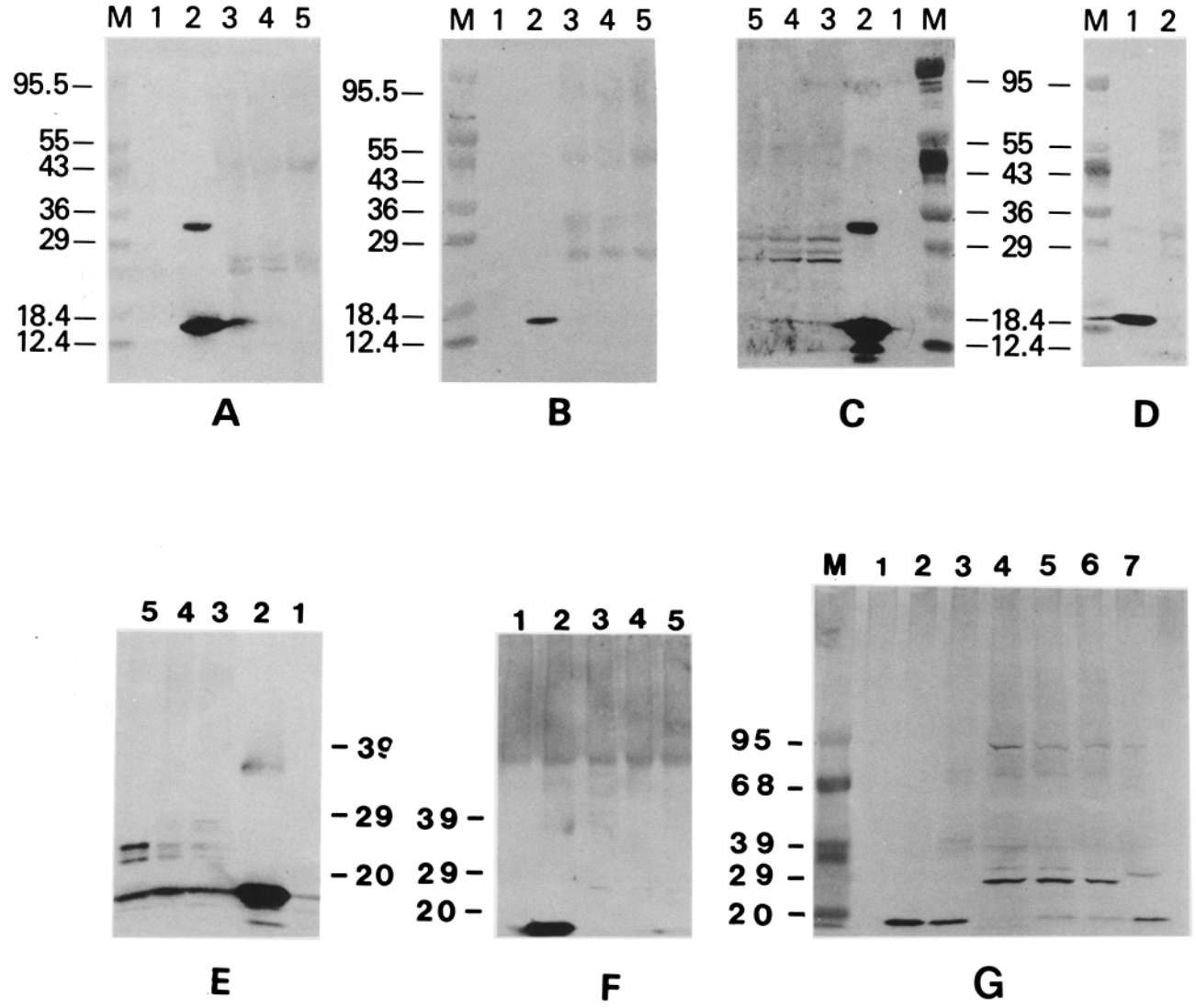

Figure 2. Western blot analysis of rat embryo extracts for bFGF. (*A*) Incubated with anti-bFGF monoclonal antibody (mAb) #78. Lane *M*, Molecular mass standards; lanes *1–5* were same as in Fig. 1 *A*. (Lane *2* illustrates the expected 18-kD band and smaller amounts of the nonreducible 35-kD dimers in this preparation of rbFGF). (*B*) Incubated with anti-bFGF mAb #98. (*C*) Incubated with anti-bFGF polyclonal antibody C135. The lanes were the same as in *A*, 26–28-kD bands predominate, and 17–18-kD bFGF bands in the crude embryo extracts (lanes *3–5*) and proteolytic fragments of the rbFGF also are shown. (*D*) Incubated with preabsorbed antibody C135. Lane *1*, human recombinant bFGF (hrbFGF) (100 ng); lane *2*, crude extract of 16-d embryo. Immunoreactive bands were significantly suppressed. (*E*) Incubation with mAb type II. Lane *1*, bovine aFGF (50 ng); lane *2*, hrbFGF (50 ng), 18-kD and faint 36-kD bands (dimer) are shown; lane *3*, 1.5 M NaCl eluate of 16-d embryo, 28-, 26-, 24-, and 18-kD bands are shown; lane *4*, 1.5 M NaCl eluate of 16-d embryo treated with Laemmli buffer with 8 M urea, 28-kD band becomes fainter; 26-, 24,- and 18-kD bands become more intense. Lane *5*, 1.5 M NaCl eluate of adult rat brain, 26-, 24-, and 18-kD bands are shown. (*F*) Incubated with anti-bFGF polyclonal antibody C135; lane *1*, bovine aFGF (50 ng); lane *2*, hrbFGF (30 ng); lanes *3–5* are same as in *C*. In 1.5 M NaCl eluate of 16-d embryo, 28-kD band and faint 14- and 18-kD bands are shown. With 8 M urea, 28-kD band becomes fainter, and 26- and 18-kD bands become more intense. In adult rat brain, 18-kD band is predominant; 24- and 28-kD bands are very faint. (*G*) Immunoblots using anti-bFGF 967 of heparin-Sepharose eluates of adult rat heart (lane *3*), 16-d rat embryo with (lane *5*) or without (lane *4*) 8 M urea in the Laemmli buffer, 17-d embryo with 8 M urea (lane *6*) and 2-wk-old rat brain (lane *7*). 28-kD band is seen only in brain and whole embryo and is disaggregated to 18-kD by 8 M urea. Lane *1*, 50 ng aFGF. Lane *2*, 50 ng bFGF. *M*, relative molecular mass standards.

(days 11–14) to later stages of development (days 15–20) (Figs. 5, *c* and *d*, and 6, *c* and *d*). The white zone showed intense staining at all stages examined. At the cellular level, staining for aFGF was positive in the migrating neuroblasts and differentiated neurons and glia, and it was negative in some cells located in the anterior horns.

In the brain, the general pattern of immunoreactivity for aFGF was similar to that described in the spinal cord (Figs. 5, *a* and *b*, and 6, *a* and *b*). The gray matter showed a progressive increase in the area positively stained and in the intensity of staining from earlier to later stages of embryonic development, while the white matter showed intense and ho-

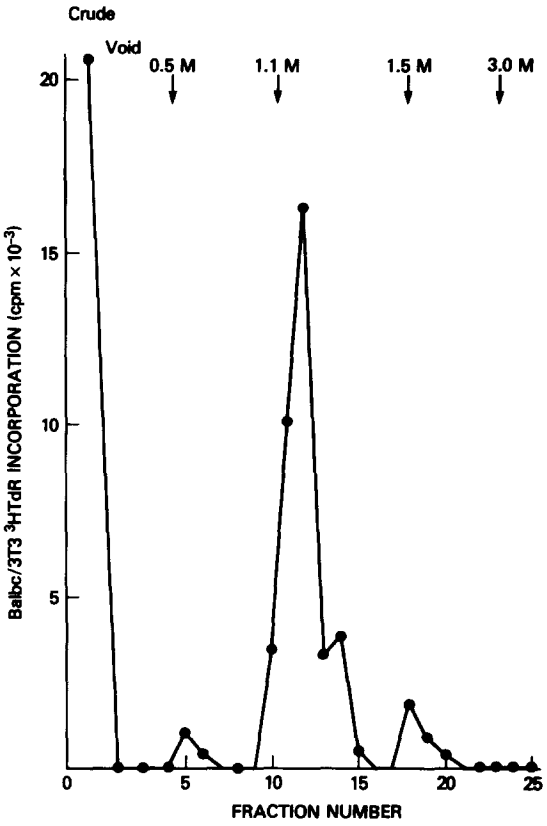

Figure 3. Mitogenicity assay for 3T3 cells of crude extracts and heparin-Sepharose affinity chromatographic fractions of rat embryos aged 16 d. Both crude extracts, 1.1- and 1.5-M fractions, exhibit mitogenicity in 3T3 cells.

mogeneous staining throughout all stages examined. In the meninges, immunostaining was also intense and homogeneous throughout all the developmental stages examined.

Eye. Immunolocalization of aFGF in the eye was examined during the later stages of development (days 16–20, Fig. 6 *a*). The vitreous body and optic nerve stained intensely at all stages examined. At day 16, the retina showed positive staining only in the cell layers that were contiguous to the vitreous body, from days 17–20, the cell layers of the retina showing positive staining which increased in parallel with the increasing number of layers. At earlier stages (day 16), the cornea showed positive staining of epithelial, stromal, and endothelial layers, but by day 19 it showed positive staining only in Bowman's and Descemet's membranes.

Heart. The developing heart stained positively for aFGF at each of the stages studied (Figs. 4 *a*, 5, *a* and *e*, and 6 *e*). However, at earlier stages (days 11–13), the intensity of staining was less in the endothelial cells of the endocardium than in the cardiac myocytes (Fig. 5 *a*). Staining was also positive in the mesenchymal cushions from which the heart valves and the roots of the pulmonary artery and the aorta develop (Fig. 4 *a*). The endothelial cells of the capillaries showed nonuniform staining for aFGF throughout development (Figs. 5 *e* and 6 *e*).

Respiratory System. In the lungs, the pattern of immunostaining for aFGF remained constant throughout all stages examined. Connective tissue within the lungs showed positive staining (Figs. 4 *a*, 5 *f*, and 7, *a* and *c*). Immunoreactivity was more intense and uniform in the cytoplasm of fibroblasts and in the extracellular matrix. The epithelium of the airways (which originates from the endoderm) remained negative at all stages examined, and the smooth muscle layers of the airways showed only faint staining (Figs 5 *f*, and 7, *a* and *c*). During development of the lungs, there is a progressive increase in the amount of bronchial epithelial tissue relative to the amount of connective tissue; thus, the lungs showed substantially less immunoreactivity at later stages (days 19–20) than at earlier stages (days 13–14, see Figs. 5 *f* and 7 *c*).

In the trachea, the pattern of immunostaining for aFGF was similar to that of the lungs (Fig. 7 *a*). The fibroblasts and extracellular matrix of the connective tissue showed the most intense immunoreactivity, while chondroblasts and

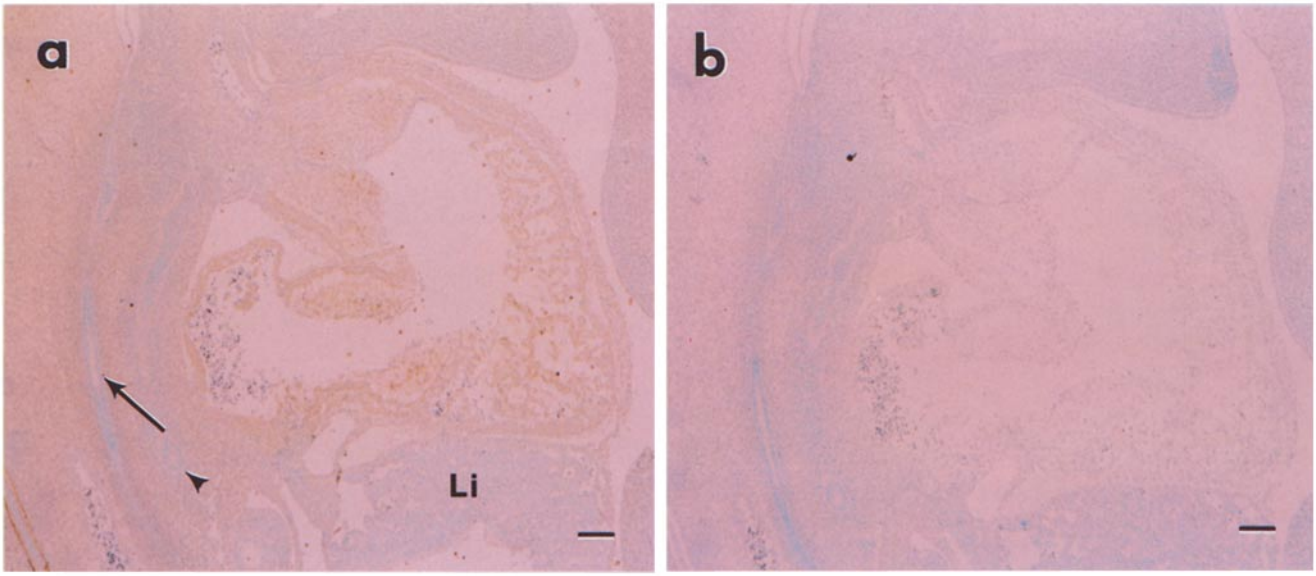

Figure 4. Sagittal sections of 15-d rat embryo. (*a*) Immunoreactive aFGF (antibody #119) is present in the heart and surrounding mesenchymal tissues, and it is absent in the liver (*Li*) and the epithelia of the digestive system (*arrow*) and respiratory system (*arrowhead*). (*b*) Immunostaining for aFGF is negative after incubation with preabsorbed Ab #119. Bars, 100 μm.

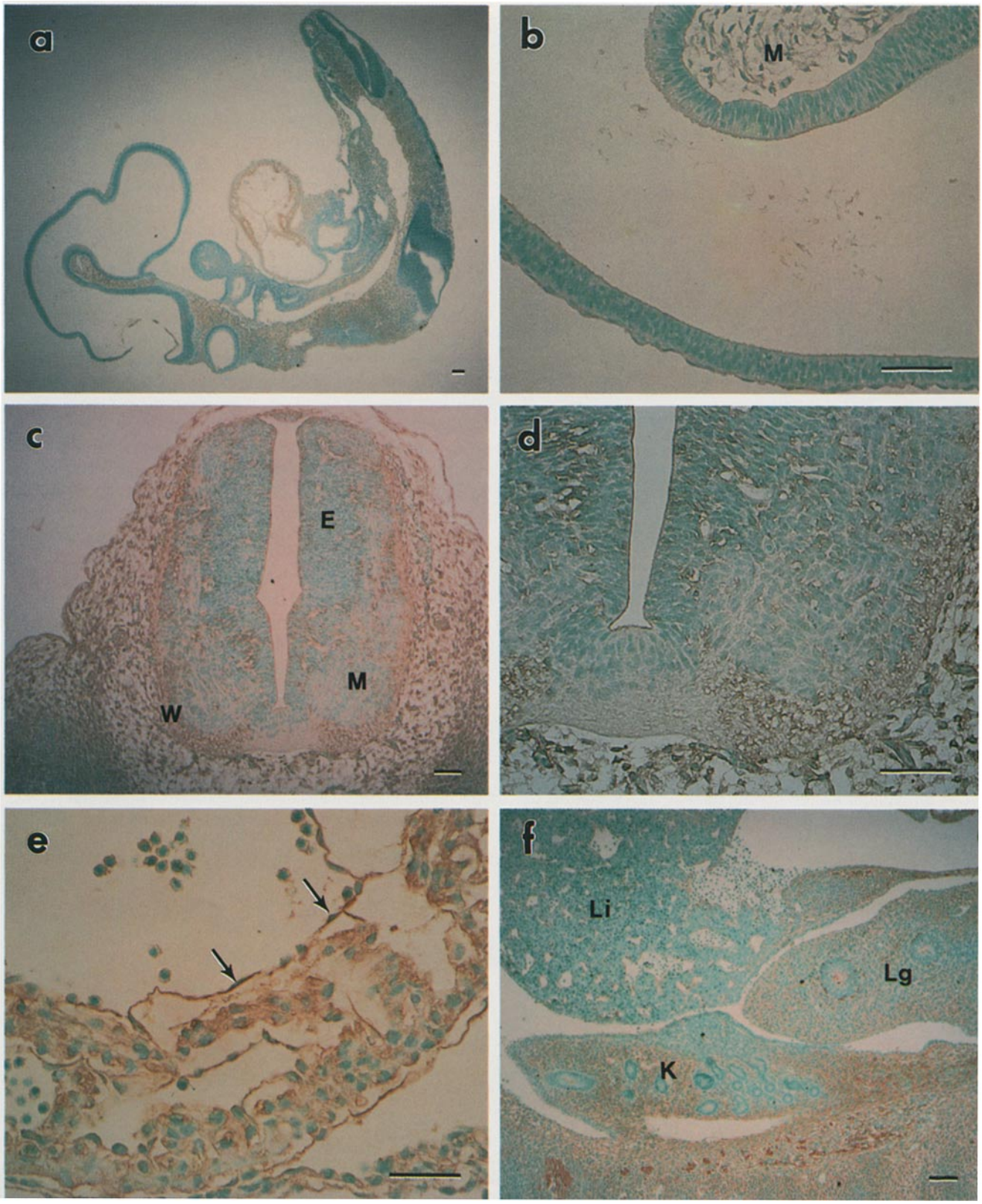

Figure 5. Immunolocalization of aFGF in 11–14-d rat embryos. (*a*) Sagittal section of 11-d embryo stained with Ab #63; positive immunostaining is seen in the heart, brain, mesenchymal tissues, and somites. (*b*) Sagittal section of 11-d embryo stained with mAb shows positive immunostaining of brain and mesenchyme (*M*); staining is more positive in the outer (more differentiated) layers of the brain. (*c*) Cross section of the spinal cord of 14-d embryo stained with Ab #63; staining is positive in the mantle zone or middle layer (*M*) and the white zone (*W*), and it is negative in the less differentiated ependyma (*E*). (*d*) Same section as in *c*, but at higher magnification; positive staining is seen in the cytoplasm of the migrating neuroblasts and the extracellular matrix. (*e*) Detail of part of *a*, showing sagittal section of the

chondrocytes within the tracheal walls showed less intense and nonuniform staining. Smooth muscle in the wall of the trachea and in the media of the vessels showed only faint staining. The tracheal epithelium showed no immunoreactivity at any of the stages examined.

Kidneys. The pattern of staining for aFGF in the kidneys remained constant throughout all stages examined (Figs. 5 *f* and 6 *c*). Connective tissue showed intense staining, while the epithelium of the tubules showed no immunoreactivity. Thus, at later stages, when the cortex and the medulla could be clearly identified, the cortex (containing a high percentage of epithelial cells) showed substantially less staining than the medulla (rich in connective tissue) (Fig. 6 *c*). The kidney capsule, which is composed of connective tissue, showed positive immunoreactivity at all stages examined.

Digestive System. In the esophagus, the connective tissue showed intense immunoreactivity for aFGF, the epithelium showed no staining, and the smooth muscle cells showed nonuniform and weak staining. The same pattern of immunostaining was present in the stomach and intestines (Fig. 6 *f*).

In the liver, the hepatocytes showed no staining throughout all stages examined (Figs. 4 *a*, 5 *f*, and 6 *f*). Only the endothelial cells of the hepatic sinusoids, veins and arteries, and foci of hematopoiesis showed positive staining (Fig. 5 *f*).

Skeleton. At early stages of embryonic development (days 11–12), the somites constituting the axial skeleton showed positive staining for aFGF, with the peptide being present in the cytoplasm of most of the cells (Fig. 5 *a*). At later stages, when somites were clearly differentiated into sclerotome, myotome, and dermatome, the chondroblasts and osteoblasts showed positive staining, while the perichondrium and the periosteum showed no immunoreactivity. The three endochondral primary ossification centers of the vertebrae, which became apparent at 15–16 d, showed intense staining, and the immunoreactivity of the ossification centers was clearly higher than that of the surrounding chondroblasts (Fig. 6 *c*).

Throughout all stages of long bone development (13–20 d), the limbs showed predominantly positive and diffuse staining for aFGF. In particular, the areas of intramembranous ossification and the contiguous osteoblasts showed intense staining. Conversely, the perichondrium and periosteum showed no immunoreactivity (Fig. 7 *b*).

Skeletal Muscle. At earlier stages (11–14 d), skeletal muscle cell precursors that were adjacent to the developing vertebrae showed positive and homogenous staining for aFGF (Fig. 5, *a* and *f*). At later stages (16–18 d), when the skeletal myoblasts could first be identified, the cytoplasm of the myoblasts also showed positive immunoreactivity (Figs. 6 *d* and 7 *b*). At later stages of development (days 18–20) the skeletal muscle showed less intense staining.

Thymus. Neither the cortex nor the medulla of the thymus showed any immunoreactivity for aFGF, throughout all stages examined. The connective tissue that forms the organ capsule and divides it into lobes, showed positive and intense staining throughout all stages examined (Fig. 7 *d*).

Comparison of Immunohistochemical Localization of aFGF and bFGF

The cellular and tissue distribution of bFGF was substantially similar to that of aFGF. Multiple antisera directed against several epitopes of bFGF gave identical results. The general distribution of immunoreactive bFGF is shown in serial sections (Fig. 7, *e* and *f*).

Discussion

Natural Forms of aFGF and bFGF

Acidic FGF is a single chain peptide composed of 140–154 amino acids and its molecular mass has been reported to vary between 15 and 18 kD, depending on the different cells, organs, and species of origin (5, 59) and extraction methods. Acidic FGF has a high degree of structural homology with bFGF, a more extensively investigated growth factor that has a range of molecular masses (18, 19, 26, 32, 45, 57). Recently, a heparin-binding immunoreactive bFGF-like protein of high molecular mass (25 kD) has been identified in extracts of adult rat liver (45). In addition, a 25-kD bFGF has been purified from guinea pig brain tissue and appears to be an NH_2-terminally extended and posttranslationally modified form of bFGF (57). In the present investigation, we identified high molecular mass forms for both aFGF and bFGF. Western blot analysis, performed on rat embryo crude extracts and heparin-bound material, using several highly specific polyclonal and monoclonal antibodies, identified 26–28-kD molecular mass forms of aFGF and 24–28-kD bFGF. Specificity is suggested by the fact that the same bands are detected by different antibodies corresponding to different residues of FGFs and are suppressed by the corresponding FGFs. The absence of high molecular forms of immunoreactive aFGF in adult brain extract indicates that the high molecular mass forms of immunoreactive aFGF (and bFGF) are developmentally regulated. Moreover these peptides were mitogenic for 3T3 cells. These appeared to be the main immunoreactive forms of the two peptides in the rat embryo.

Genomic clones and cDNA of bFGF predict a 17.8-kD (155 amino acids) gene product, based on the presence of a single putative translation-initiating ATG codon. In a previous study, multiple molecular forms of bFGF (17.8, 22.5, 23.1 and 24.2 kD) were identified in the human hepatoma cell line SK-HEP-1 (18). In that study, an SK-HEP-1 bFGF cDNA was used to show that in vitro transcription–translation, as well as in vivo COS-1 cell expression experiments, result in the synthesis of multiple bFGF protein species. Selective mutagenesis of this cDNA demonstrated that the translation of the 17.8-kD protein is initiated at the previously predicted AUG codon, while the translation of the 22.5-, 23.1-, and 24.2-kD proteins is initiated at CUG codons. Therefore, it would appear that the higher molecular mass forms of bFGF are the colinear NH_2-terminal exten-

heart of an 11-d embryo stained with Ab #63; staining is positive in the cytoplasm of the myocytes and in the extracellular matrix, and it is nonuniform in the endothelial cells (*arrows*), some cells showing positive and other cells negative staining. (*f*) Sagittal section of 14-d embryo stained with Ab #119; staining is positive in the mesenchyme of the lungs (*Lg*) and kidneys (*K*), and it is negative in the liver (*Li*) and in the epithelium of the lungs and kidneys. Bars, 50 μm.

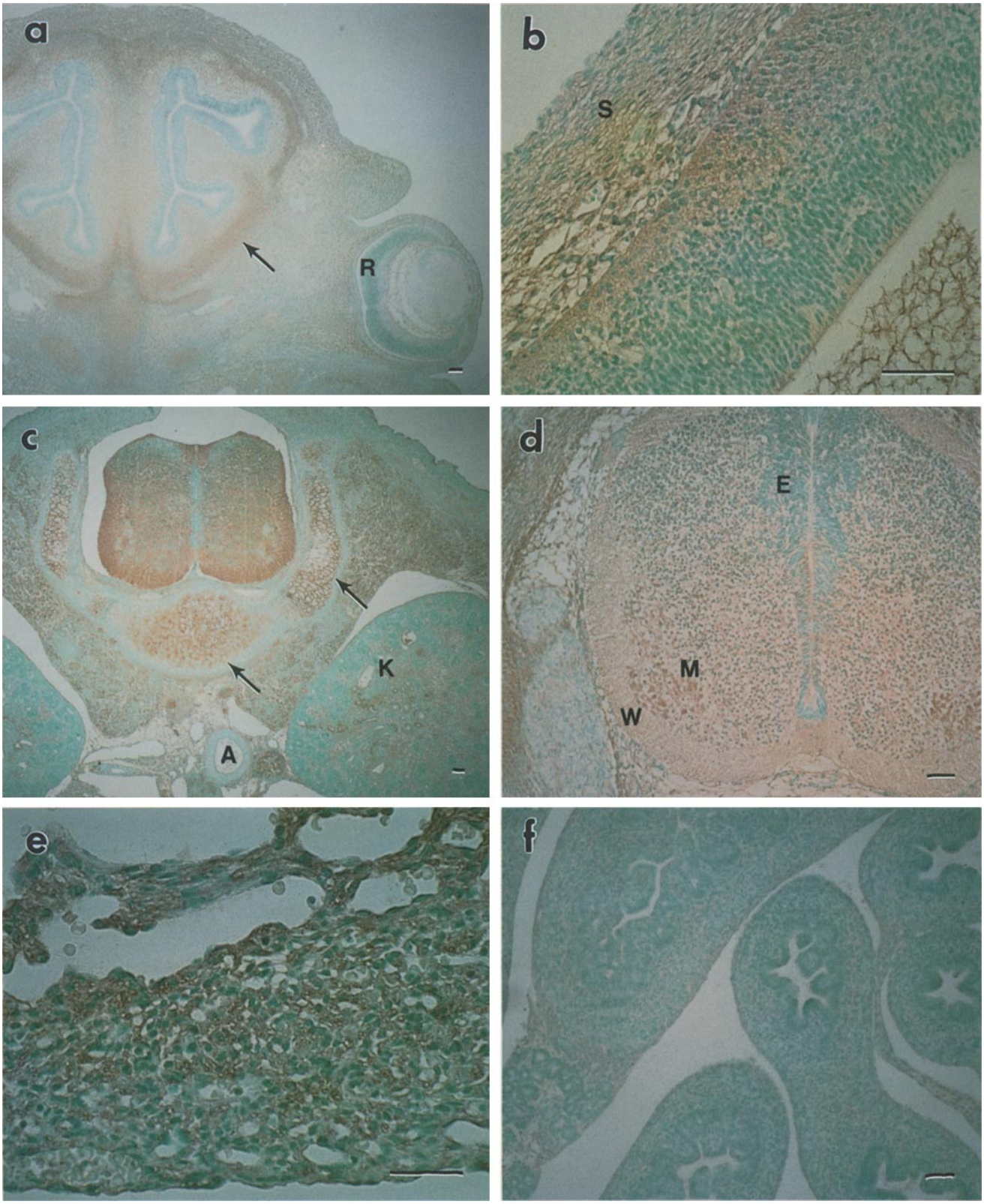

Figure 6. Immunolocalization of aFGF in rat embryos at later stages of development (16–20 d). (*a*) Cross section of brain and eye of 19-d embryo stained with Ab #63. Immunostaining is positive in the brain cortex (*arrow*), in the layers of the retina (*R*) contiguous to the vitreous body, in the capillary network and anterior lens epithelium. (*b*) Sagittal section of brain of 17-d embryo stained with mAb; staining is more positive in the outer (more differentiated) layers than in the inner (less differentiated) layers of the brain, and it is also positive in the skin (*S*). (*c*) Cross section of 19-d embryo at kidney level stained with Ab #119; staining is positive in the spinal cord, ossification centers of the vertebrae (*arrows*), and mesenchymal tissue of the kidneys (*K*); it is faint in the media of the aorta (*A*) and negative in the cortex of the kidneys. (*d*) Cross section of the spinal cord of 16 d embryo stained with AB #63: staining is positive in the mantle

sions of the 17.8-kD bFGF. In contrast, the aFGF gene has an inframe stop codon just 5′ to the start codon. Thus, neither gene predicts products of >25 kD. Adding 8 M urea at 100°C before SDS-PAGE under denaturing conditions dissociated the embryonic 28-kD bFGF to the expected 24- and 18-kD forms. The identities of the 28-kD immunoreactive aFGF and bFGF found when SDS-PAGE is performed without urea are not known. Addition of 8 M urea may dissociate some small binding protein, yielding the expected forms of aFGF and bFGF. The roles of high molecular mass aFGF and bFGF are not known. Recent data suggest a nuclear role for these forms (46).

Immunohistochemical Localization of aFGF

Previous observations support the hypothesis that aFGF and bFGF stimulate proliferation and differentiation of embryonic tissues (36, 55, 61). However, the embryonic distribution of aFGF has not been reported. In the present study, immunoreactive aFGF was widely distributed and regulated in tissues of neuroectodermal and mesodermal origin.

Central Nervous System. Both FGFs have previously been extracted from brain tissue (5, 15, 48) but their biological functions in the development of the central nervous system remain unknown. There is in vitro evidence that these growth factors stimulate proliferation and differentiation of nervous cells, and favorably influence their survival. Basic FGF has been shown to enhance neurite growth and survival in hippocampal, mesencephalic, dopaminergic, and GABAergic neurons, and in PC 12 cells (2, 13, 16, 38, 42, 60), and it also has been reported to have mitogenic effects on glial and Schwann cells, chromaffin cells, and embryonic neuroblasts which later express cholinergic differentiation (10, 22). Acidic FGF is mitogenic for Schwann cells (10), chemotactic for astroglia and enhances process formation in retinal sensory neurons (53).

While the cellular localization of bFGF in the central nervous system of the adult rat has been reported previously (14), that of aFGF has never been described and the embryonic neural distributions of both FGFs are unknown. In the present study, immunoreactive aFGF was widely distributed in the cytoplasm of the migrating neuroblasts, neurons, astroglia, and glia and was not identified in the undifferentiated and proliferating neuroepithelial cells that are adjacent to the lumen of the central tube of the spinal cord and to the lumen of the ventricles (23). We also identified changes in the distribution of immunoreactive aFGF that paralleled the changes in cell differentiation that accompany organogenesis. For example, while the differentiating cells of the gray matter and white matter showed progressively more intense and homogenous staining during development, the undifferentiated cells of the ependyma showed no immunoreactivity throughout all the stages examined. The progressive increase in aFGF in the central nervous system is more consistent with a role in synapse formation, transmission or trophism than in proliferation per se. The accumulation of apparently extracellular aFGF coincides with, and may contribute to, capillary invasion in the central nervous system. These findings suggest that aFGF plays an active role in the morphogenesis of the central nervous system in the rat embryo.

In the anterior horns of the spinal cord, the majority of motor neurons die after failing to establish synapses with skeletal myocytes (33). Motor neurons with processes showed intense staining for aFGF, while cells with few or no processes showed no staining. This finding suggests that the loss of aFGF might also have a role as a signal for programmed cell death.

Eye. Acidic FGF and bFGF have previously been isolated from adult and embryo retina (4, 27, 41, 43). In this report, we describe the coexpression of aFGF and bFGF in the optic nerve and in the innermost developing layers of the retina, probably corresponding to the future nerve fiber layer and ganglion cell layers, and perhaps the inner plexiform and nuclear layers. Until several weeks after birth, and subsequent opening of the eyelids, these layers are not well differentiated and the retina is poorly vascularized (27). These facts may explain the differences between our observations and those reported in adult retina, where aFGF mRNA and peptide are widely distributed, whereas bFGF mRNA is reported only in the photoreceptor layer (7, 42), although the peptide is also found in the cultured retinal pigment epithelium (51). In our study, both peptides were associated with the process of retinal differentiation, as indicated by the development of axons and dendrites.

We also localized aFGF and bFGF to the epithelium of the anterior of the lens, especially in the extracellular matrix. aFGF has previously been extracted from adult bovine lens (7) and the lens epithelium of the 6-wk-old rat expresses aFGF but not bFGF mRNA (42). Both FGFs are mitogenic for lens epithelial cells in vitro (41).

In the present study we localized aFGF and bFGF to all the layers of the cornea. Gospodarowicz found bFGF to be mitogenic for corneal epithelium and endothelium (26). Naji et al. localized aFGF mRNA to the basal epithelial cells of the anterior cornea of the 6-wk-old rat, but found no expression of bFGF in these cells (43). Caruelle et al. localized aFGF immunoreactivity in the basal cells but not in Bowman's or Descemet's membranes (7), where Folkman et al. had found bFGF immunoreactivity (20). These adult distributions clearly differ from those we observed in the embryonic cornea.

Tissues of Mesodermal Origin. Although exogenous aFGF is mitogenic for mesenchymal cells in vitro and induces mesoderm when added to *Xenopus* explant, aFGF could not be detected in *Xenopus* oocytes and early embryos whereas bFGF was detected (37, 55, 56). Thus, the role of endogenous aFGF in the development of mesodermal tissues remains unclear. In the present investigation, immunoreactive aFGF was identified in all mesodermal tissues throughout embryonic development. At later stages of development, however, immunoreactivity for aFGF became less intense in some lin-

zone or middle layer (*M*) and the white zone (*W*), and it is negative in the less differentiated ependyma (*E*). (*e*) Section of the myocardium of 20-d embryo stained with Ab #63; staining is positive in the myocytes, in most endothelial cells of the endocardium and capillaries, and in the extracellular matrix. (*f*) Section of the digestive system of 18-d embryo stained with Ab #63; staining is positive in the mesenchymal tissue and negative in the epithelium. Bars, 50 μm.

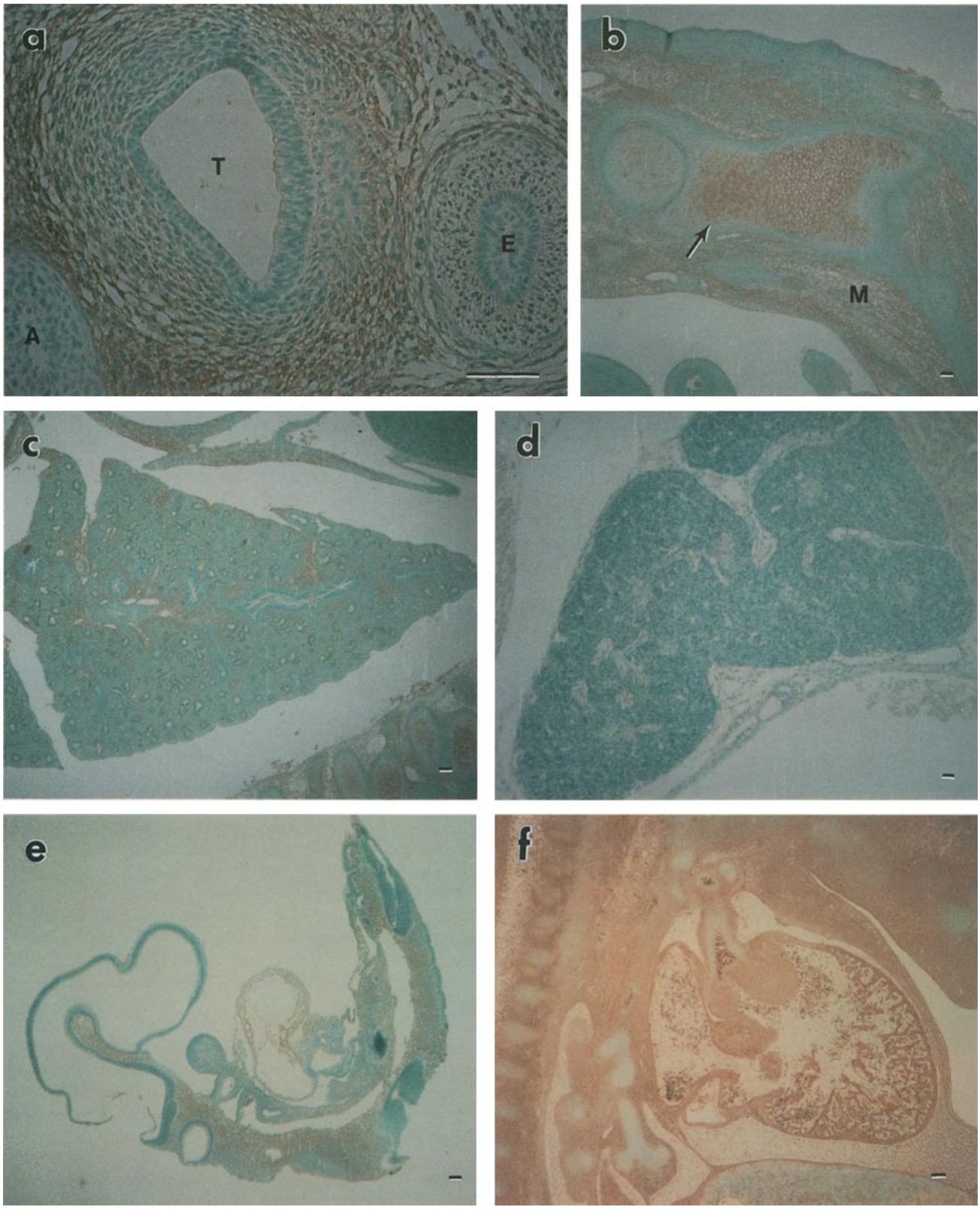

Figure 7. Immunolocalization of aFGF in several organs at late stages of development (17–19 d) (*a–d*), and general distribution of immunoreactive bFGF in 11- and 15-d rat embryo (*e* and *f*). (*a*) Cross section of 17-d embryo at neck level stained with Ab #63; staining is intense in the connective tissue surrounding the trachea (*T*) and esophagus (*E*); It is faint in the chondrocytes of the trachea and in the smooth muscle of the media of a large artery (*A*); it is negative in the epithelium of trachea and esophagus. (*b*) Hind limb of 18-d embryo stained with Ab #119; staining is intense in the ossification center (*arrow*) and is also positive in the skeletal muscle (*M*). (*c*) Lungs of 18-d embryo stained with Ab #119; staining is positive in the mesenchymal tissue of the lungs and is negative in the epithelium of airways. (*d*) Thymus

eages, such as the skeletal muscle cells. Although it is not yet known whether this indicates a decline in the synthesis and use of aFGF, it is noteworthy that bFGF delays skeletal myoblast differentiation in vitro (9) and receptors for aFGF and bFGF decline in number with differentiation of non-neural tissues (44).

In other tissues of mesodermal origin, such as the bones, the pattern of immunoreactivity for aFGF also showed progressive changes during development. Immunostaining was less intense and homogenous in the differentiating and proliferating chondroblasts than in the undifferentiated mesenchymal cells, and staining was absent in the perichondrium and periosteum. At later stages, however, immunostaining became again intensely positive in the ossification centers. These findings suggest that aFGF, which has previously been extracted from bone and cartilage (28, 49), may have different roles in bone development, including stimulation of chondroblast and osteoblast proliferation, as well as stimulation of the angiogenesis that precedes ossification (3, 6, 24).

aFGF has previously been extracted from kidneys (21, 47). In the present study, immunoreactivity for aFGF in the kidneys, like in the bones, appeared to be inversely related to cell differentiation. For example, cells that are highly differentiated, such as the epithelial cells of the glomeruli and tubules of the cortex, showed no immunoreactivity for aFGF. Conversely, less differentiated mesenchymal cells of the medulla showed intense and uniform staining. These findings are interesting in light of previous observations showing that the mesenchyme triggers the differentiation of renal primordia into nephrons (50).

Immunoreactive aFGF was also noted in many endothelial cells. The angiogenic effect of adding FGFs to the avascular cornea is well known (5, 19, 26). However, many factors are angiogenic and the role of endogenous bFGF has yet to be clarified. aFGF has not been detected in most endothelial cells (19, 26, 34), with one exception (3). We did not examine the early stages of vasculogenesis, but during angiogenic invasion of developing brain, spinal cord, and bone intense endothelial aFGF immunostaining was noted. Some cells were unstained, perhaps due to restriction of aFGF expression to specific stages of the cell cycle; or the absence of this growth factor could denote endothelial cells destined for programmed cell death in the stage when some capillaries regress and others develop into arterioles and venules.

The differences in the distribution of immunoreactive aFGF that we identified in cells and tissues of mesodermal origin have important implications, since they suggest that aFGF's regulatory effects may be tissue specific.

Tissues of Endodermal Origin. In higher organisms, the epithelial cells that cover the inner surfaces of the respiratory and digestive systems and the distal portion of the urinary system (bladder and urethra) originate from the endoderm. The epithelial cells of the thymus and thyroid, and the functional cellular elements of all the digestive glands (including pancreas and liver) are also of endodermal origin. At all stages examined, the cells of endodermal origin were devoid of immunoreactive aFGF. However, aFGF was expressed in the mesoderm-derived tissues (such as the connective tissue) of these organs. Moreover, embryonic endodermal derivatives may have FGF receptors, since aFGF is mitogenic for hepatocytes in vitro (31, 44). In addition, in vivo infusion of neutralizing antisera to bFGF has been shown to disrupt the development of endoderm-derived tissues (39). The absence of FGFs in endoderm-derived tissues seems to contrast with the mounting evidence that bFGF is one of the signals by which the endoderm induces mesoderm formation in *Xenopus* (36, 55). Since there are substantial differences in gastrulation between toad and rat, it is possible that neither bFGF nor aFGF play a role in rat gastrulation, or that these two peptides are not present in the endoderm, but stored in the ectoderm and activated by a substance released by the endoderm. Therefore, although we could not identify immunoreactive aFGF in tissues of endodermal origin, these previous observations suggest that aFGF may have a role in the growth and differentiation of these tissues.

Comparison of Immunohistochemical Localization of aFGF and bFGF

Previous observations indicate that, like aFGF, bFGF may play important roles in differentiation and growth of embryonic tissues of neuroectodermal and mesodermal origin (55, 56). In the present investigation, we have compared the cellular and tissue distribution of bFGF with that of aFGF in rat embryos at different stages. Each of the several antibodies used in the present study identified a very similar cellular and tissue distribution of these peptides during development, and each peptide was widely distributed in tissues of neuroectodermal and mesodermal origin. The similarities in the distribution of immunoreactive aFGF and bFGF we identified in the rat embryo are consistent with their similar mitogenic and chemotactic effects on cells of mesodermal and neuroectodermal origin in vitro (5, 26). In addition, these similarities are consistent with the results of previous studies of 18-d rat embryo (25).

Conclusions

The findings of the present study indicate that 26–28-kD immunoreactive aFGF and bFGF are probably the main natural forms of these peptides in the rat embryo. In addition, our comparative analysis of the cellular and tissue distribution of immunoreactive aFGF and bFGF demonstrates that these peptides have a widespread and similar distribution in neuroectodermal and mesodermal tissues of the rat embryo. Finally, our results show progressive and similar changes in the distribution of these peptides during embryonic development, and such changes appear to be associated with the processes of cell growth, migration, and differentiation.

The authors would like to acknowledge the expert editorial assistance of Maude Atcheson.

of 19-d embryo stained with Ab #63; staining is negative in this organ. (*e*) Serial sagittal section of 11-d embryo stained with Ab #773 for bFGF; staining is positive in the heart and surrounding mesenchymal tissues, the distribution of staining is superimposable to that of aFGF in Fig. 5 *a*. (*f*) Serial section stained with Ab #967 for bFGF; distribution of staining is similar to that of aFGF (Fig. 4 *a*). Bars, 50 μm.

Received for publication 24 August 1990 and in revised form 24 May 1991.

References

1. Abraham, J. A., J. L. Whang, A. Tumolo, A. Mergia, J. Friedman, D. Gospodarowicz, and J. C. Fiddes. 1986. Human basic fibroblast growth factor: nucleotide sequence and genomic organization. *EMBO (Eur. Mol. Biol. Organ.) J.* 5:2523–2528.
2. Anderson, K. J., D. Dam, S. Lee, and C. W. Cotman. 1988. Basic fibroblast growth factor prevents death of lesioned cholinergic neurons in vivo. *Nature (Lond.).* 332:360–361.
3. Baird, A., and P. A. Walicke. 1989. Fibroblast growth factors. *Br. Med. Bull.* 45:438–452.
4. Baird, A., F. Esch, D. Gospodarowicz, and R. Guillemin. 1985. Retina- and eye-derived endothelials cell growth factors; partial molecular characterization and identity with acidic and basic fibroblast growth factors. *Biochemistry.* 24:7855–7859.
5. Burgess, W. H., and T. Maciag. 1989. The heparin-binding (fibroblast) growth factor family of proteins. *Annu. Rev. Biochem.* 58:575–606.
6. Canalis, E., J. Lorenzo, W. Burgess, and T. Maciag. 1987. Effects of endothelial cell growth factor on bone remodeling in vitro. *J. Clin. Invest.* 79:52–58.
7. Caruelle, D., B. Groux-Moscatelli, A. Gaudric, C. Sesteir, G. Coscas, J. P. Caruelle, and D. Barritault. 1989. Immunological study of acidic fibroblast growth factor (aFGF) distribution in the eye. *J. Cell. Biochem.* 39:117–128.
8. Casscells, W., E. Speir, J. Sasse, M. Klagsbrun, P. Allen, M. Lee, B. Calvo, M. Chiba, L. Haggroth, J. Folkman, and S. E. Epstein. 1990. Isolation, characterization, and localization of heparin-binding growth factors in the heart. *J. Clin. Invest.* 85:433–441.
9. Clegg, C. H., T. A. Linkhart, B. B. Olwin, and S. D. Hauschka. 1987. Growth factor control of skeletal muscle differentiation: commitment to terminal differentiation occurs in G1 phase and is repressed by fibroblast growth factor. *J. Cell Biol.* 105:949–956.
10. Davis, J. B., and P. Stroobant. 1990. Platelet-derived growth factors and fibroblast growth factors are mitogens for rat Schwann cells. *J. Cell Biol.* 110:1353–1360.
11. Delli Bovi, P., A. M. Curatola, F. G. Kern, A. Greco, M. Ittmann, and C. Basilico. 1987. An oncogene isolated by transfection of Kaposi's sarcoma DNA encodes a growth factor that is a member of the FGF family. *Cell.* 50:729–737.
12. Dickson, C., and G. Peters. 1987. Potential oncogene product related to growth factors. *Nature (Lond.).* 326:833.
13. Dreyer, D. 1989. Basic fibroblast growth factor prevents ontogenetic neuron death in vivo. *Neurosci. Lett.* 99:35–38.
14. Emoto, N., A. -M. Gonzalez, P. A. Walicke, E. Wada, D. M. Simmons, S. Shimasaki, and A. Baird. 1989. Basic fibroblast growth factor (FGF) in the central nervous system: identification of specific loci of basic FGF expression in the rat brain. *Growth Factors.* 2:21–29.
15. Esch, F., N. Ueno, A. Baird, F. Hill, L. Denoroy, N. Ling, D. Gospodarowicz, and R. Guillemin. 1985. Primary structure of bovine brain acidic fibroblast growth factor (FGF). *Biochem. Biophys. Res. Commun.* 133:554–562.
16. Ferrari, G., M. C. Minozzi, G. Toffano, A. Leon, and S. D. Skaper. 1989. Basic fibroblast growth factor promotes the survival and development of mesencephalic neurons in culture. *Dev. Biol.* 133:140–147.
17. Finch, P. W., J. S. Rubin, T. Miki, D. Ron, and S. A. Aaronson. 1989. Human KGF is FGF-related with properties of a paracrine effector of epithelial cell growth. *Science (Wash. DC).* 245:752–755.
18. Florkiewicz, R. Z., and A. Sommer. 1989. Human basic fibroblast growth factor gene encodes four polypeptides: three initiate translation from non-AUG codons. *Proc. Natl. Acad. Sci. USA.* 86:3978–3981.
19. Folkman, J., and M. Klagsbrun. 1987. Angiogenic factors. *Science (Wash. DC).* 235:442–447.
20. Folkman, J., M. Klagsbrun, J. Sasse, M. G. Wadzinski, D. Ingber, and I. Vlodavsky. 1988. A heparin-binding angiogenic protein, basic fibroblast growth factor, is stored within basement membrane. *Am. J. Pathol.* 130:393–400.
21. Gautschi-Sova, P., Z. -P. Jiang, M. Frater-Schröder, and P. Bölen. 1987. Acidic fibroblast growth factor is present in nonneural tissues: isolation and chemical characterization from bovine kidney. *Biochemistry.* 26: 5844–5847.
22. Gensburger, C., G. Labourdette, and M. Sensenbrenner. 1987. Brain basic fibroblast growth factor stimulates the proliferation of rat neuronal precursor cells in vitro. *FEBS (Fed. Eur. Biochem. Soc.) Lett.* 217:1–5.
23. Gilbert, S. F. 1988. Early vertebrate development: neurulation and ectoderm. Early vertebrate development: mesoderm and endoderm. *In* Developmental Biology. 2nd Ed. S. F. Gilbert, editor. Sinaver Associates, Sunderland, Massachusetts. 152–244.
24. Globus, R. K., P. Patterson-Buckendahl, and D. Gospodarowicz. 1988. Regulation of bovine bone cell proliferation by fibroblast growth factor and transforming growth factor β. *Endocrinology.* 123:98–105.
25. Gonzalez, A., M. Buscalia, M. Ong, and A. Baird. 1990. Distribution of basic fibroblast growth factor in the 18-d rat fetus: localization in the basement membranes of diverse tissues. *J. Cell Biol.* 110:753–765.
26. Gospodarowicz, D. 1989. Fibroblast growth factor. *Crit. Rev. Oncogen.* 1:1–26.
27. Hanneken, A., G. A. Lutty, D. S. McLeod, F. Robey, A. K. Harvey, and L. M. Hjelmelund. 1989. Localization of basic fibroblast growth factor to the developing capillaries of the bovine retina. *J. Cell. Physiol.* 138:115–120.
28. Hauschka, P. W., A. E. Mavrakos, M. D. Iafrati, S. E. Doleman, and M. Klagsbrun. 1986. Growth factors in bone matrix: isolation of multiple types by affinity chromatography on heparin-sepharose. *J. Biol. Chem.* 261:12665–12674.
29. Hebel, R., and M. W. Stromberg. 1986. Anatomy and Embryology of the Laboratory Rat. BioMed. Verlag. *Wörthsee.* 271 pp.
30. Hèbert, J. M., C. Basilico, M. Goldfarb, O. Haub, and G. R. Martin. 1990. Isolation of cDNAs encoding four mouse FGF family members and characterization of their expression patterns during embryogenesis. *Dev. Biol.* 138:454–463.
31. Houck, K. A., R. Zarnegar, S. J. Muga, and G. K. Michalopoulos. 1989. Acidic fibroblast growth factor (HBGF-1) stimulates DNA synthesis in primary rat hepatocyte cultures. *J. Cell. Physiol.* 143:129–132.
32. Iberg, N., S. Rogelj, P. Fanning, and M. Klagsbrun. 1989. Purification of 18- and 22-KD forms of basic fibroblast growth factor from rat cells transformed by the *ras* oncogene. *J. Biol. Chem.* 264:19951–19955.
33. Jacobson, M. 1978. Developmental Neurobiology. 2nd Ed. Plenum Publishing Corp., New York. 562 pp.
34. Joseph-Silverstein, J., S. A. Consigli, K. M. Lyser, and C. Ver Pault. 1989. Basic fibroblast growth factor in the chick embryo: immunolocalization to striated muscle cells and their precursors. *J. Cell Biol.* 108:2459–2466.
35. Kimelman, D., and M. Kirschner. 1987. Synergistic induction of mesoderm by FGF and TGF-beta and the identification of an mRNA coding for FGF in the early *Xenopus* embryo. *Cell.* 51:869–877.
36. Kimelman, D., and M. Kirschner. 1989. An antisense mRNA directs the covalent modification of the transcript encoding fibroblast growth factor in *Xenopus* oocytes. *Cell.* 59:687–696.
37. Kimelman, D., J. A. Abraham, T. Haaparanta, T. M. Palisi, and M. W. Kirschner. 1988. The presence of fibroblast growth factor in the frog egg: its role as a natural mesoderm inducer. *Science (Wash. DC).* 242:1053–1056.
38. Lipton, S. A., J. A. Wagner, R. D. Madison, and P. A. D'Amore. 1988. Acidic fibroblast growth factor enhances regeneration of processes by postnatal mammalian retinal ganglion cells in culture. *Proc. Natl. Acad. Sci. USA.* 84:2388–2392.
39. Liu, L., and C. S. Nicoll. 1988. Evidence for a role of basic fibroblast growth factor in rat embryonic growth and differentiation. *Endocrinology.* 123:2027–2031.
40. Marics, I., J. Adelaide, F. Raybaud, M. -G. Mattei, F. Coulier, J. Planche, O. de Lapeyriere, and D. Birnbaum. 1989. Characterization of the HST-related FGF.6 gene, a new member of the fibroblast growth factor gene family. *Oncogene.* 4:335–340.
41. Mascarelli, F., D. Raulais, M. F. Counis, and Y. Courtois. 1987. Characterization of acidic and basic fibroblast growth factors in brain, retina, and vitreous of the chick embryo. *Biochem. Biophys. Res. Commun.* 146:478–486.
42. Morrison, R. S., A. Sharma, J. De Vellis, and R. A. Bradshaw. 1986. Basic fibroblast growth factor supports the survival of cerebral cortical neurons in primary culture. *Proc. Natl. Acad. Sci. USA.* 83:7537–7541.
43. Naji, S., T. Matsuo, E. Koyama, T. Yamaai, T. Nohno, N. Matsuo, and S. Taniguchi. 1990. Expression pattern of acidic and basic fibroblast growth factor genes in adult rat eyes. *Biochem. Biophys. Res. Commun.* 168:343–349.
44. Olwin, B. B., and S. D. Hauschka. 1990. Fibroblast growth factor receptor levels decrease during chick embryogenesis. *J. Cell Biol.* 110:503–509.
45. Presta, M., M. Statuto, M. Rusnati, P. Dell'Era, and G. Ragnotti. 1989. Characterization of an Mr 25,000 basic fibroblast growth factor form in adult, regenerating, and fetal rat liver. *Biochem. Biophys. Res. Commun.* 164:1182–1189.
46. Renko, M., N. Quarto, T. Morimoto, and D. B. Rifkin. 1990. Nuclear and cytoplasmic localization of different basic fibroblast growth factor species. *J. Cell Physiol.* 144:108–114.
47. Risau, W., and P. Ekblom. 1986. Production of a heparin-binding angiogenesis factor by the embryonic kidney. *J. Cell Biol.* 103:1101–1107.
48. Risau, W., P. Gautschi-Sova, and P. Böhlen. 1988. Endothelial cell growth factors in embryonic and adult chick brain are related to human acidic fibroblast growth factor. *EMBO (Eur. Mol. Biol. Organ.) J.* 7:959–962.
49. Sasse, J., R. Sullivan, and M. Klagsbrun. 1987. Purification of cartilage-derived growth factors. *Methods Enzymol.* 146:320–325.
50. Saxen, L. 1975. Embryonic induction. *Clin. Obstet. Gynecol.* 18:149–175.
51. Schweigerer, L., B. Malerstein, G. Neufeld, and D. Gospodarowicz. 1987. Basic FGF is synthesized in cultured retinal pigment epithelial cells. *Biochem. Biophys. Res. Commun.* 143:934–940.
52. Seed, J., B. B. Olwin, and S. D. Hauschka. 1988. Fibroblast growth factor levels in the whole embryo and limb bud during chick development. *Dev. Biol.* 128:50–57.
53. Senior, R. M., S. S. Huang, G. L. Griffin, and J. S. Huang. 1986. Brain-

derived growth factor is a chemoattractant for fibroblasts and astroglial cells. *Biochem. Biophys. Res. Commun.* 141:67–72.

54. Seno, M., M. Iwane, R. Sasada, N. Moriya, T. Kurokawa, and K. Igarashi. 1989. Monoclonal antibodies against human basic fibroblast growth factor. *Hybridoma.* 8:209–221.
55. Slack, J. M. W., and H. V. Isaacs. 1989. Presence of basic fibroblast growth factor in the early *Xenopus* embryo. *Development (Camb.).* 105:147–153.
56. Slack, J., B. Darlington, H. Heath, and S. Godsave. 1987. Mesoderm induction in early *Xenopus* embryos by heparin-binding growth factors. *Nature (Lond.).* 326:197–200.
57. Sommer, A., D. Moscatelli, and D. B. Rifkin. 1989. An amino-terminally extended and post-translationally modified form of a 25 kD basic fibroblast growth factor. *Biochem. Biophys. Res. Commun.* 160:1267–1274.
58. Taira, M., T. Yoshida, K. Miyagawa, H. Sakamoto, M. Terada, and T. Sugimura. 1987. cDNA sequence of human transforming gene hst and identification of the coding sequence required for transforming activity. *Proc. Natl. Acad. Sci. USA.* 84:2980–2984.
59. Thomas, K. A., M. Rios-Candelore, G. Gimenez-Gallego, J. DiSalvo, C. Bennett, J. Rodkey, and S. Fitzpatrick. 1985. Pure brain-derived acidic fibroblast growth factor is a potent angiogenic vascular endothelial cell mitogen with sequence homology to interleukin 1. *Proc. Natl. Acad. Sci. USA.* 82:6409–6413.
60. Wagner, J. A., and P. A. D'Amore. 1986. Neurite outgrowth induced by an endothelial cell mitogen isolated from retina. *J. Cell Biol.* 103:1363–1367.
61. Whitman, M., and D. A. Melton. 1989. Growth factors in early embryogenesis. *Annu. Rev. Cell Biol.* 5:93–117.
62. Zhan, X., B. Bates, X. Hu, and M. Goldfarb. 1988. The human FGF-5 oncogene encodes a novel protein related to fibroblast growth factors. *Mol. Cell Biol.* 8:3487–3495.